# THE NEURO-SYMBOLIC CONCEPT LEARNER: INTERPRETING SCENES, WORDS, AND SENTENCES FROM NATURAL SUPERVISION

**Anonymous authors**
Paper under double-blind review

## ABSTRACT

We propose the Neuro-Symbolic Concept Learner (NS-CL), a model that learns visual concepts, words, and semantic parsing of sentences without explicit supervision on any of them; instead, our model learns by simply looking at images and reading paired questions and answers. Our model builds an object-based scene representation and translates sentences into executable, symbolic programs. To bridge the learning of two modules, we use a neuro-symbolic reasoning module that executes these programs on the latent scene representation. Analog to the human concept learning, given the parsed program, the perception module learns visual concepts based on the language description of the object being referred to. Meanwhile, the learned visual concepts facilitate learning new words and parsing new sentences. We use curriculum learning to guide searching over the large compositional space of images and language. Extensive experiments demonstrate the accuracy and efficiency of our model on learning visual concepts, word representations, and semantic parsing of sentences. Further, our method allows easy generalization to new object attributes, compositions, language concepts, scenes and questions, and even new program domains. It also empowers applications including visual question answering and bidirectional image-text retrieval.

## 1 INTRODUCTION

Humans are capable of learning visual concepts by jointly understanding vision and language (Fazly et al., 2010; Chrupała et al., 2015; Gauthier et al., 2018). Take the example shown in Figure 1-I. Imagine that a human with no prior knowledge of colors, is presented with the images of the red and green cubes paired with the questions and answers. She can easily identify the differences in certain component of the visual appearance (e.g., color in this case) of the objects and align the component to the corresponding word in the question and answer (`Red` and `Green`). Other single-object level attributes (e.g., shape) can also be learned in a similar fashion. Starting from there, a human is also able to inductively learn the correspondence between visual concepts and word semantics (e.g., spatial relations and referential expressions) Figure 1-II, and unravel compositional logic from complex questions assisted by the learned visual concepts Figure 1-III (Abend et al., 2017).

Motivated by the way humans jointly perceive visual concepts and understand languages through a joint reasoning process (Gauthier et al., 2018), we propose a neuro-symbolic concept learner (NS-CL) that jointly learns visual perception, words, and semantic language parsing based on a visual question answering (VQA) setup. We employ a visually-grounded semantic parser for translating questions into executable programs, and a neural-based perception module that extracts object-level representations from the scene. A symbolic program executor then reads out the perceptual representation of objects, classifies their attributes/relations, and executes the program to obtain an answer.

Our model learns from natural supervision (i.e., images and QA pairs) via curriculum learning. It starts by learning representations of individual objects from short questions (e.g., What's the color of the cylinder?) on simple scenes ($\leq$3 objects). It then learns relational concepts by leveraging object-level concepts to interpret object referrals (e.g., Is there a box right of a cylinder?). The model then iteratively adapts to more complex scenes and highly compositional questions.

Our model recovers an object-based representation for visual scenes. Meanwhile, based on the learned visual representations, we propose a visually-grounded semantic parsing approach to find

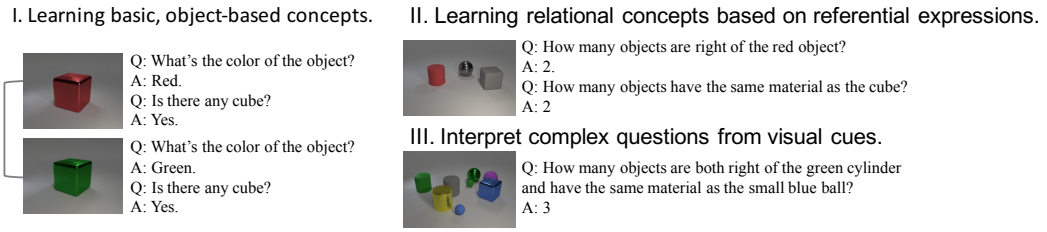


Figure 1: Humans learn visual concepts, words, and semantic parsing jointly and incrementally. **I.** Learning visual concepts (red *vs*. green) starts from looking at simple scenes, reading simple questions, and reasoning over contrastive examples (Fazly et al., 2010). **II.** Afterwards, we can interpret referential expressions based on the learned object-based concepts, and learn relational concepts (e.g., on the right of, the same material as). **III** Finally, we can interpret complex questions from visual cues by exploiting the compositional structure.

the correspondence between word semantics and visual concepts. It also learns to perform semantic parsing on sentences with *zero* program annotations.

These disentangled and structural representations enable interpretable and robust visual reasoning. Our neuro-symbolic approach achieves state-of-the-art performance on the CLEVR dataset Johnson et al. (2017a), and more importantly, it naturally learns visual and language concepts, which support combinatorial generalization w.r.t. the complexity of the scene and the programs (e.g., the depth of the program tree). By modeling attributes such as `Color` and `Shape` as neural operators, our model suggests solutions to visual compositional generalization, demonstrated on CLEVR-CoGenT (Johnson et al., 2017a), and to incremental concept learning. The learned visual concepts can be easily applied into other domains such as image-caption retrieval by only changing program specification.

## 2 Related Work

Our model is related to research on joint learning from visual data and natural language. In particular, there are many papers that learn visual concepts from descriptive visually-grounded languages, such as image-captioning or visually-grounded question-answer pairs (Kiros et al., 2014; Mao et al., 2016; Vendrov et al., 2016; Ganju et al., 2017), dense language descriptions for scenes (Johnson et al., 2016), video-captioning (Donahue et al., 2015) and video-text alignment (Zhu et al., 2015).

Visual question answering (VQA) stands out as it requires understanding both visual content and language. The state-of-the-art approaches usually use neural attentions (Malinowski & Fritz, 2014; Chen et al., 2015; Yang et al., 2016; Xu & Saenko, 2016). Beyond question answering, Johnson et al. (2017a) proposed the CLEVR (VQA) dataset to diagnose reasoning models. CLEVR contains synthetic visual scenes and questions generated from latent programs. Table 1 compares our model with state-of-the-art visual reasoning models (Andreas et al., 2016; Suarez et al., 2018; Santoro et al., 2017) along four directions: visual features, semantics, inference, and the requirement of extra labels.

For visual representations, Johnson et al. (2017b) encoded visual scenes into a convolutional feature map for program operators. Mascharka et al. (2018); Hudson & Manning (2018) used attention as intermediate representations for transparent program execution. Recently, Yi et al. (2018) explored an interpretable, object-based visual representation for visual reasoning. It performs well, but requires fully-annotated scenes during training. Our model also adopts an object-based visual representation, but the representation is learned only based on natural supervision (questions and answers).

Anderson et al. (2018) also proposed to represent the image as a collection of convolutional object features and gained substantial improvements on VQA. Their model encodes questions with neural networks and answers the questions by question-conditioned attention over the object features. In contrast, NS-CL parses question inputs into programs and executes them on object features to get the answer. This makes the reasoning process interpretable and supports combinatorial generalization over quantities (e.g., counting objects). Our model also learns general visual concepts and their association with symbolic representations of language. These learned concepts can then be explicitly interpreted and deployed in other vision-language applications such as image caption retrieval.

There are two types of approaches in semantic sentence parsing for visual reasoning: implicit programs as conditioned neural operations (e.g., conditioned convolution and dual attention) (Perez et al., 2017; Hudson & Manning, 2018) and explicit programs as sequences of symbolic tokens (Johnson et al., 2017b; Mascharka et al., 2018). Explicit programs gain better interpretability, but usually

| Models | Visual Features | Semantics | Extra Labels | | Inference |
|---|---|---|---|---|---|
| | | | # Prog. | Attr. | |
| FiLM (Perez et al., 2017) | Convolutional | Implicit | 0 | No | Feature Manipulation |
| IEP (Johnson et al., 2017b) | Convolutional | Explicit | 700K | No | Feature Manipulation |
| MAC (Hudson & Manning, 2018) | Attentional | Implicit | 0 | No | Feature Manipulation |
| Stack-NMN (Hu et al., 2018) | Attentional | Implicit | 0 | No | Attention Manipulation |
| TbD (Mascharka et al., 2018) | Attentional | Explicit | 700K | No | Attention Manipulation |
| NS-VQA (Yi et al., 2018) | Object-Based | Explicit | 0.2K | Yes | Symbolic Execution |
| NS-CL | Object-Based | Explicit | 0 | No | Symbolic Execution |

Table 1: Comparison with other frameworks on the CLEVR VQA dataset, w.r.t. visual features, implicit or explicit semantics and supervisions.

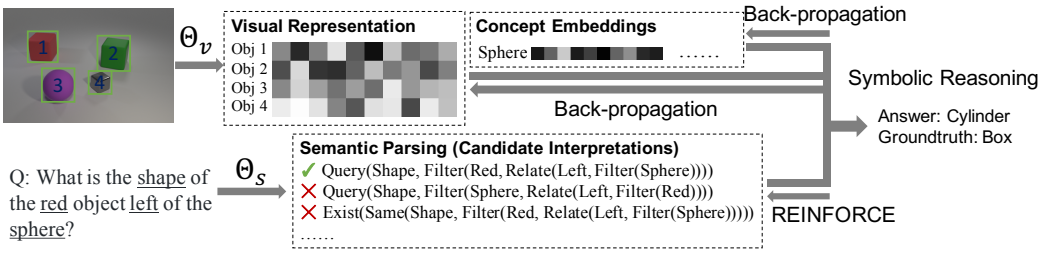


Figure 2: We propose to use neural symbolic reasoning as a bridge to jointly learn visual concepts, words, and semantic parsing of sentences.

require extra supervision such as ground-truth program annotations for training. This restricts their application. We propose a visually-grounded semantic parsing approach to parse questions in natural languages into explicit programs with *zero* program annotations. Given the semantic parsing of questions into programs, Yi et al. (2018) proposes a purely symbolic executor for the inference of the answer in the logic space. Compared with theirs, we propose a quasi-symbolic executor for VQA.

Our work is also related to learning interpretable and disentangled representations for visual scenes using neural networks. Kulkarni et al. proposed convolutional inverse graphics networks for learning and inferring pose of faces, while Yang et al. (2015) learned disentangled representation of pose of chairs from images. Wu et al. (2017) proposes the neural scene de-rendering framework as an inverse process of any rendering process. Siddharth et al. (2017); Higgins et al. (2018) learned disentangled representations using deep generative models. In contrast, we propose an alternative interpretable and disentangled representations learning approach through joint reasoning with language.

## 3 NEURO-SYMBOLIC CONCEPT LEARNER

We present our neuro-symbolic concept learner, which uses a symbolic reasoning process to learn visual concepts, words, and semantic parsing of sentences without explicit annotations for any of them. We first use a visual perception module to construct an object-based representation for a scene, and run a semantic parsing module to translate a question into an executable program. We then apply a quasi-symbolic program executor to infer the answer based on the scene representation. We use paired images, questions, and answers to jointly train the visual and language modules.

Shown in Figure 2, given an input image, the visual perception module detects objects in the scene and extracts a deep, latent representation for each of them. The semantic parsing module translates an input question in natural language into an executable program in a domain specific language (DSL). The generated programs have a hierarchical structure of symbolic, functional modules, each fulfilling a specific operation over the scene representation. The explicit program semantics enjoys compositionality, interpretability, and generalizability.

The program executor executes the program upon the derived scene representation and answers the question. Our program executor works in a symbolic and deterministic manner. This feature ensures a transparent execution trace of the program. Our program executor has a fully differentiable design w.r.t. the visual representations and concept embeddings, which can be updated using standard back-propagation during training.

### 3.1 MODEL DETAILS

**Visual perception.** Shown in Figure 2, given the input image, we use a Mask R-CNN pipeline (He et al., 2017) to generate object proposals for all objects. The bounding box for each single object

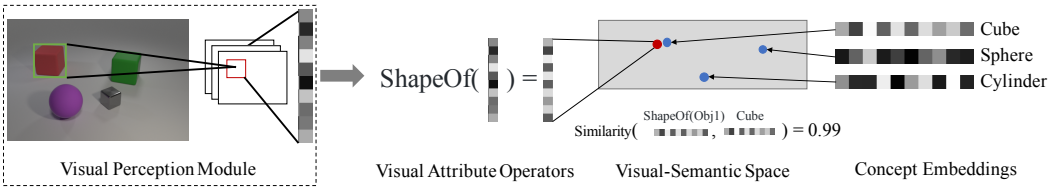


Figure 3: We treat attributes such as `Shape` and `Color` as neural operators. The operators map object representations into a visual-semantic space. We use similarity-based metric to classify objects.

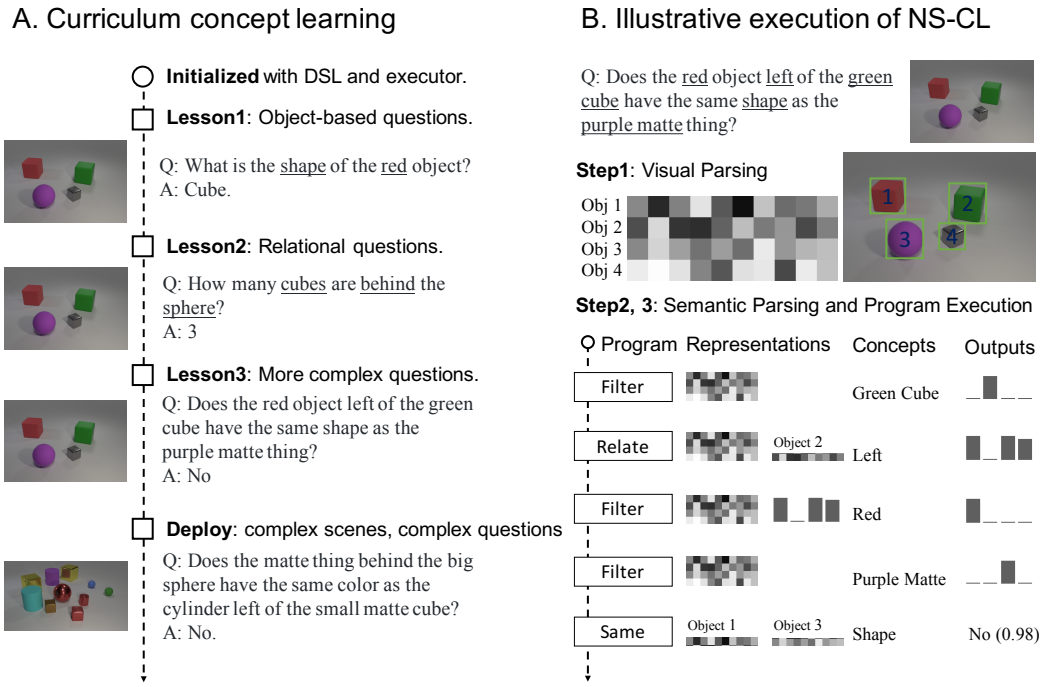


Figure 4: **A.** Demonstration of the curriculum learning of visual concepts, words, and semantic parsing of sentences by watching images and reading paired questions and answers. Scenes and questions of different complexities are illustrated to the learner in an incremental manner. **B.** Illustration of our neuro-symbolic inference model for VQA. The perception module begins with parsing visual scenes into object-based deep representations, while the semantic parser parse sentences into executable programs. A symbolic execution process bridges two modules.

paired with the original image is then sent to a ResNet-34 (He et al., 2015) to extract the region-based (by RoI Align) and image-based features respectively. We concatenate them to represent each object. Here, the inclusion of the representation of the full scene adds the contextual information, which is essential for the inference of relative attributes such as size or spatial position.

**Concept quantization.** Visual reasoning requires determining an object's attributes (e.g., its color or shape). We assume each visual attribute (e.g., shape) contains a set of possible visual concept (e.g., `Cube`). In NS-CL, visual attributes are implemented as neural operators (Nagarajan & Grauman, 2018), mapping the object representation into an attribute-specific embedding space. Figure 3 shows an inference of the shape of an object. Visual concepts that belong to the shape attribute, including `Cube`, `Sphere` and `Cylinder`, are represented as vectors in this shared space. These concept vectors are also learned along the process. We measure the cosine distances $\langle \cdot, \cdot \rangle$ between these vectors to decide the shape of the object. Specifically, we compute the probability that an object $o_i$ is a cube by $\sigma\left(\langle \text{ShapeOf}(o_i), v_{\texttt{Cube}} \rangle - \gamma\right) / \tau$, where $\text{ShapeOf}(\cdot)$ denotes the neural operator, $v_{\texttt{Cube}}$ the concept embedding of `Cube` and $\sigma$ the Sigmoid function. $\gamma$ and $\tau$ are scalar constants for scaling and shifting the values of similarities. We classify relational concepts (e.g., `Left`) between a pair of objects similarly, except that we concatenate the visual representations for both objects to form a representation of the pair.

**DSL and semantic parsing.** The semantic parsing module translates a natural language question into an executable program with a hierarchy of primitive operations, represented in a domain-specific language (DSL) designed for VQA. The DSL covers a set of fundamental operations for visual

reasoning, such as filtering out objects with certain concepts or query the attribute of an object. The operations share the same input and output interface, and thus can be compositionally combined to form programs of any complexity. We include a complete specification of the DSL used by our framework in the Appendix A.

Our semantic parser generates the hierarchies of latent programs in a sequence to sequence manner (Sutskever et al., 2014). We use a bidirectional GRU (Cho et al., 2014) to encode an input question, which outputs a fixed-length embedding of the question. A decoder based on GRU cells is applied to the embedding, and recovers the hierarchy of operations as the latent program.

**Quasi-symbolic program execution.** Given the latent program recovered from the question in natural language, a symbolic program executor executes the program and derives the answer based on the object-based visual representation. Our program executor is a collection of deterministic functional modules designed to realize all logic operations specified in the DSL. Figure 4(B) shows an illustrative execution trace of a program.

To make the execution differentiable w.r.t. visual representations, we represent the intermediate results in a probabilistic manner. Specifically, a set of objects is represented by a real-valued mask over all objects in the scene. Each element, $\texttt{Mask}_i \in [0, 1]$ represents the probability that the $i$-th object of the scene belongs to the set. For example, shown in Figure 4(B), the first `Filter` operation outputs a mask of length $4$ (there are in total 4 objects in the scene), with each element representing the probability that the corresponding object is selected out (i.e., the probability that each object is a green cube). The output "mask" on the objects will be fed into the next module (`Relate` in this case) as input and the execution of programs continues. The last module outputs the final answer to the question. We refer interested readers to Appendix C for the implementation of operators.

### 3.2 Training paradigm

**Optimization objective.** The optimization objective of NS-CL is composed of two parts: concept learning and language understanding. Our goal is to find the optimal parameters $\Theta_v$ of the visual perception module and $\Theta_s$ of the semantic parsing module, to maximize the likelihood of answering the question $Q$ correctly:

$$\Theta_v, \Theta_s \leftarrow \arg\max_{\Theta_v, \Theta_s} \mathbb{E}_P[\Pr[A = \text{Executor}(\text{Perception}(S; \Theta_v), P)]], \tag{1}$$

where $P$ denotes the program, $A$ the answer, and $S$ the scene. The expectation is taken over $P \sim \text{SemanticParse}(Q; \Theta_s)$.

Recall the program executor is fully differentiable w.r.t. the visual representation. We compute the gradient w.r.t. $\Theta_v$ as $\nabla_{\Theta_v} \mathbb{E}_P[D_{\text{KL}}(\text{Executor}(\text{Perception}(S; \Theta_v), P) \| A)]$. We use REINFORCE (Williams, 1992) to optimize the semantic parser $\Theta_s$ via $\nabla_{\Theta_s} = \mathbb{E}_P[r \cdot \log \Pr[P | \text{SemanticParse}(Q; \Theta_s)]]$, where the reward $r = 1$ if the answer is correct and 0 otherwise. We also use off-policy search to reduce the variance of REINFORCE, the detail of which can be found at Appendix B.

**Curriculum visual concept learning.** Motivated by human concept learning as in Figure 1, we employ a curriculum learning approach to help joint optimization. We heuristically split the training samples into four stages (Figure 4(A)): first, learning object-level visual concepts; second, learning relational questions; third, learning more complex questions with perception modules fixed; fourth, joint fine-tuning of all modules. Empirical experiments show that this is essential to the learning of our neuro-symbolic concept learner. We include more technical details in Appendix D.

## 4 Experiments

We demonstrate the following advantages of our NS-CL. First, it learns visual concepts with remarkable accuracy; second, it allows data-efficient visual reasoning on the CLEVR dataset (Johnson et al., 2017a); third, it generalizes well to new attributes, visual composition, and language domains.

We train NS-CL on 5K images (<10% of CLEVR's 70K training images). We generate 20 questions for each image for the entire curriculum learning process.

### 4.1 Visual concept learning

**Classification-based concept evaluation.** Our model treats attributes as neural operators that map latent object representations into an attribute-specific embedding space (Figure 3). We evaluate the

| | Visual | Mean | Color | Mat. | Shape | Size |
|---|---|---|---|---|---|---|
| IEP | Conv. | 90.6 | 91.0 | 90.0 | 89.9 | 90.6 |
| MAC | Attn. | 95.9 | 98.0 | 91.4 | 94.4 | 94.2 |
| TbD (hres.) | Attn. | 96.5 | 96.6 | 92.2 | 95.4 | 92.6 |
| NS-CL | Obj. | **98.7** | **99.0** | **98.7** | **98.1** | **99.1** |

Table 2: We also evaluate the learned visual concepts using a diagnostic question set containing simple questions such as "How many `red` objects are there?". NS-CL outperforms both convolutional and attentional baselines. The suggested object-based visual representation and symbolic reasoning approach perceives better interpretation of visual concepts.

| Model | Visual | Accuracy (100% Data) | Accuracy (10% Data) |
|---|---|---|---|
| TbD | Attn. | 99.1 | 54.2 |
| TbD-Object | Obj. | 84.1 | 52.6 |
| TbD-Mask | Attn. | 99.0 | 55.0 |
| MAC | Attn. | 98.9 | 67.3 |
| MAC-Object | Obj. | 79.5 | 51.2 |
| MAC-Mask | Attn. | 98.7 | 68.4 |
| NS-CL | Obj. | **99.2** | **98.9** |

Table 3: We compare different variants of baselines for a systematic study on visual features and data efficiency. Using only 10% of the training images, our model is able to achieve a comparable results with the baselines trained on the full dataset. See the text for details.

concept quantization of objects in the CLEVR validation split. Our model can achieve near perfect classification accuracy ($\sim$99%) for all object properties, suggesting it effectively learns generic concept representations. The result for spatial relations is relatively lower. This is because CLEVR does not have direct queries on the spatial relation between objects, so spatial relation concepts can only be learned indirectly.

**Count-based concept evaluation.** The SOTA methods do not provide interpretable representation on individual objects (Johnson et al., 2017a; Hudson & Manning, 2018; Mascharka et al., 2018) . To evaluate the visual concepts learned by such models, we generate a synthetic question set. The diagnostic question set contains simple questions as the following form: "How many `red` objects are there?". We evaluate the performance on all concepts appeared in the CLEVR dataset.

Table 2 summarizes the results compared with strong baselines, including methods based on convolutional features (Johnson et al., 2017b) and those based on neural attentions (Mascharka et al., 2018; Hudson & Manning, 2018). Our approach outperforms IEP by a significant margin (8%) and attention-based baselines by $>$2%, suggesting object-based visual representations and symbolic reasoning helps to interpret visual concepts.

### 4.2 Data-efficient and interpretable visual reasoning

NS-CL jointly learns visual concepts, words and semantic parsing by watching images and reading paired questions and answers. It can be directly applied to VQA.

Table 4 summarizes results on the CLEVR validation split. Our model achieves the state-of-the-art performance among all baselines using zero program annotations, including MAC (Hudson & Manning, 2018) and FiLM (Perez et al., 2017). Our model achieves comparable performance with the strong baseline TbD-Nets (Mascharka et al., 2018), whose semantic parser is trained using 700K programs in CLEVR (ours need 0). The recent NS-VQA model from Yi et al. (2018) achieves better performance on CLEVR; however, their system requires annotated visual attributes and program traces during training, while our NS-CL needs no extra labels.

Our model also recovers the underlying programs of questions accurately ($> 99.9\%$ accuracy). Our visual perception module is pre-trained on ImageNet (Deng et al., 2009). Without pre-training, the concept learning accuracies drop by 0.2% on average and the QA accuracy drops by 0.5%. Our model can also detect ambiguous or invalid programs and indicate exceptions. Please see Appendix E for more details. NS-CL can also be applied to other visual reasoning testbeds. Please refer to Appendix F.1 for our results on the Minecraft dataset (Yi et al., 2018).

For a systematic study on visual features and data efficiency, we implement two variants of the baseline models: TbD-Object and MAC-Object. Inspired by (Anderson et al., 2018), instead of the input image, TbD-Object and MAC-Object take a stack of object features as input. TbD-Mask and MAC-Mask integrate the masks of objects by using them to guide the attention over the images.

Table 3 summarizes the results. Our model outperforms all baselines on data efficiency. This comes from the full disentanglement of visual concept learning and symbolic reasoning: how to execute program instructions based on the learned concepts is programmed in NS-CL. TbD-Object and MAC-Object demonstrate inferior results in our experiments. We attribute this to the design of model architectures and provide a detailed analysis in Appendix E.3. Although TbD-Mask and MAC-Mask

| Model | Prog. Anno. | Overall | Count | Cmp. Num. | Exist | Query Attr. | Cmp. Attr. |
|---|---|---|---|---|---|---|---|
| Human | N/A | 92.6 | 86.7 | 86.4 | 96.6 | 95.0 | 96.0 |
| NMN | 700K | 72.1 | 52.5 | 72.7 | 79.3 | 79.0 | 78.0 |
| N2NMN | 700K | 88.8 | 68.5 | 84.9 | 85.7 | 90.0 | 88.8 |
| IEP | 700K | 96.9 | 92.7 | 98.7 | 97.1 | 98.1 | 98.9 |
| DDRprog | 700K | 98.3 | 96.5 | 98.4 | 98.8 | 99.1 | 99.0 |
| TbD | 700K | **99.1** | **97.6** | **99.4** | **99.2** | **99.5** | **99.6** |
| RN | 0 | 95.5 | 90.1 | 93.6 | 97.8 | 97.1 | 97.9 |
| FiLM | 0 | 97.6 | 94.5 | 93.8 | 99.2 | 99.2 | 99.0 |
| MAC | 0 | 98.9 | 97.2 | **99.4** | **99.5** | 99.3 | **99.5** |
| NS-CL | 0 | **98.9** | **98.2** | 99.0 | 98.8 | **99.3** | 99.1 |

Table 4: Our model outperforms all baselines using no program annotations. It achieves comparable results with models trained by full program annotations such as TbD.

| Model | Test | | | |
|---|---|---|---|---|
| | Split A | Split B | Split C | Split D |
| MAC | 97.3 | N/A | 92.9 | N/A |
| IEP | 96.1 | 92.1 | 91.5 | 90.9 |
| TbD | 98.8 | 94.5 | 94.3 | 91.9 |
| NS-CL | **98.9** | **98.9** | **98.7** | **98.8** |

Figure 5: We test the combinatorial generalization w.r.t. the number of objects in scenes and the complexity of questions (i.e. the depth of the program trees). We makes four split of the data containing various complexities of scenes and questions. Our object-based visual representation and explicit program semantics enjoys the best (and almost-perfect) combinatorial generalization compared with strong baselines.

do not perform better than the originals, we find that using masks to guide the attention speeds up the training.

Besides achieving a competitive performance on the visual reasoning testbeds, by leveraging both object-based representation and symbolic reasoning, out model learns fully interpretable visual concepts: see Appendix G for qualitative results on various datasets.

### 4.3 Generalization to new attributes and compositions

**Generalizing to new visual compositions.** The CLEVR-CoGenT dataset is designed to evaluate models' ability to generalize to new visual compositions. It has two splits: Split A only contains gray, blue, brown and yellow cubes, but red, green, purple, and cyan cylinders; split B imposes the opposite color constraints on cubes and cylinders. If we directly learn visual concepts on split A, it overfits to classify shapes based on the color, leading to a poor generalization to split B.

Our solution is based on the idea of seeing attributes as operators. Specifically, we jointly train the concept embeddings (e.g., `Red`, `Cube`, etc.) as well as the semantic parser on split A, keeping pre-trained, frozen attribute operators. As we learn distinct representation spaces for different attributes, our model achieves an accuracy of 98.8% on split A and 98.9% on split B.

**Generalizing to new visual concepts.** We expect the process of concept learning can take place in an incremental manner: having learned 7 different colors, humans can learn the 8-th color incrementally and efficiently. To this end, we build a synthetic split of the CLEVR dataset to replicate the setting of incremental concept learning. Split A contains only images without any purple objects, while split B contains images with at least one purple object. We train all the models on split A first, and finetune them on 100 images from split B. We report the final QA performance on split B's validation set. All models use a pre-trained semantic parser on the full CLEVR dataset.

Our model performs a $93.9\%$ accuracy on the QA test in Split B, outperforming the convolutional baseline IEP (Johnson et al., 2017b) and the attentional baseline TbD (Mascharka et al., 2018) by $4.6\%$ and $6.1\%$ respectively. The acquisition of `Color` operator brings more efficient learning of new visual concepts.

### 4.4 Combinatorial generalization to new scenes and questions

Having learned visual concepts on small-scale scenes (containing only few objects) and simple questions (only single-hop questions), we humans can easily generalize the knowledge to larger-scale scenes and to answer complex questions. To evaluate this, we split the CLEVR dataset into four parts: **Split A** contains only scenes with less than 6 objects, and questions whose latent programs having a depth less than 4; **Split B** contains scenes with less than 6 objects, but arbitrary questions; **Split C** contains arbitrary scenes, but restricts the program depth being less than 4; **Split D** contains arbitrary scenes and questions. Figure 6 shows some illustrative samples.

As VQA baselines are unable to count a set of objects of arbitrary size, for a fair comparison, all programs containing the "count" operation over $> 6$ objects are removed from the set. For methods using explicit program semantics, the semantic parser is pre-trained on the full dataset and

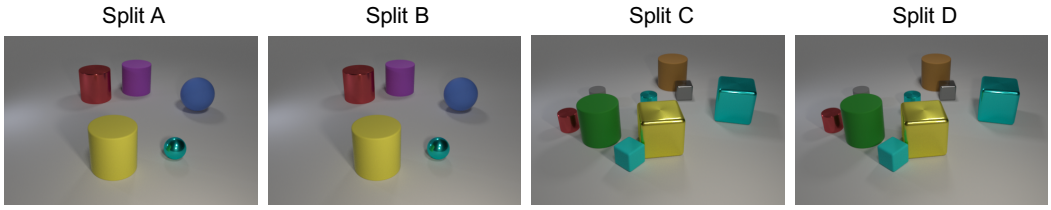


**Q**: What's the shape of the big yellow thing?

**Q**: What size is the cylinder that is left of the cyan thing that is in front of the big sphere?

**Q**: What's the shape of the big yellow thing?

**Q**: What size is the cylinder that is left of the cyan thing that is in front of the gray cube?

Figure 6: Samples collected from four splits in Section 4.3 for illustration. Models are trained on split A but evaluated on all splits for testing the combinatorial generalization.

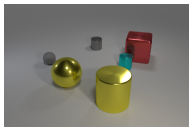

**Caption**: There is a big yellow cylinder in front of a gray object.

(a) An illustrative pair of image and caption in our synthetic dataset.

| Model | Retrieval Accuracy |
|---|---|
| IEP | 95.5 |
| TbD | **97.0** |
| NS-CL | 96.9 |

(b) Image-caption retrieval accuracy on a subset of data. Our model archives comparable results with VQA baselines.

| Model | Retrieval Accuracy |
|---|---|
| CNN-LSTM | 68.9 |
| NS-CL | **97.0** |

(c) Image-caption retrieval accuracy on the full dataset. Our model outperforms baselines and requires no extra training or fine-tuning of the visual perception module.

Table 5: We introduce a new simple DSL for image-caption retrieval to evaluate how well the learned visual concepts transfer. Due to the difference between VQA and caption retrieval, VQA baselines are only able to infer the result on a partial set of data. The learned object-based visual concepts can be directly transferred into the new domain for free.

fixed. Methods with implicit program semantics (Hudson & Manning, 2018) learn an entangled representation for perception and reasoning, and cannot trivially generalize to more complex programs. We only use the training data from the Split A and then quantify the generalization ability on other three splits. Shown in Table 5, our NS-CL leads to almost-perfect generalization to larger scenes and more complex questions, outperforming all baselines by at least $4\%$ in QA accuracy.

### 4.5 Extending to other program domain

The learned visual concepts can also be used in other domains such as image retrieval. With the visual scenes fixed, the learned visual concepts can be directly transferred into the new domain. We only need to learn the semantic parsing of natural language into the new DSL.

We build a synthetic dataset for image retrieval and adopt a DSL from scene graph–based image retrieval (Johnson et al., 2015). The dataset contains only simple captions: "There is an <object A> <relation> <object B>." (e.g., There is a box right of a cylinder). The semantic parser learns to extract corresponding visual concepts (e.g., `box`, `right`, and `cylinder`) from the sentence. The program can then be executed on the visual representation to determine if the visual scene contains such relational triples.

For simplicity, we treat retrieval as classifying whether a relational triple exists in the image. This functionality cannot be directly implemented on the CLEVR VQA program domain, because questions such as "Is there a box right of a cylinder" can be ambiguous if there exist multiple cylinders in the scene. Due to the entanglement of the visual representation with the specific DSL, baselines trained on CLEVR QA can not be directly applied to this task. For a fair comparison with them, we show the result in Table 5b on a subset of the generated image-caption pairs where the underlying programs have no ambiguity regarding the reference of object B. A separate semantic parser is trained for the VQA baselines, which translates captions into a CLEVR QA-compatible program (e.g., `Exist(Filter(Box, Relate(Right, Filter(Cylinder))).`

Table 5c compares our NS-CL against typical image-text retrieval baselines on the full image-caption dataset. Without any annotations of the sentence semantics, our model learns to parse the captions into the programs in the new DSL. It outperforms the CNN-LSTM baseline by 30%.

### 4.6 Extending to natural images and language

We further conduct experiments on MS-COCO (Lin et al., 2014) images. Results are presented on the VQS dataset (Gan et al., 2017). VQS contains a subset of images and questions from the original

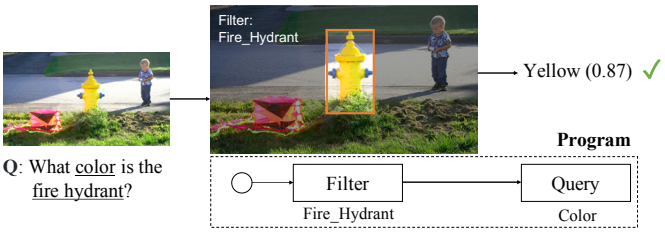


| Model | Accuracy |
|---|---|
| MLP | 43.9 |
| MAC | **46.2** |
| NS-CL | 44.3 |

Figure 7: **Left**: An example image-question pair from the VQS dataset and the corresponding execution trace of NS-CL. **Right**: Results on the VQS test set. Our model achieves a comparable results with the baselines.

Figure 8: Concepts learned from VQS, including object categories, attributes, and relations.

VQA 1.0 dataset (Antol et al., 2015). All questions in the VQS dataset can be visually grounded: each question is associated with multiple image regions, annotated by humans as essential for answering the question. Figure 7 illustrates an execution trace of NS-CL on VQS.

We use a syntactic dependency parser to extract programs and concepts from language (Andreas et al., 2016; Schuster et al., 2015). The object proposals and features are extracted from models pre-trained on the MS-COCO dataset and the ImageNet dataset, respectively. Illustrated in Figure 7, our model shows competitive performance on QA accuracy, comparable with the MLP baseline (Jabri et al., 2016) and the MAC network (Hudson & Manning, 2018). Additional illustrative execution traces of NS-CL are in Appendix G. Beyond answering questions, NS-CL effectively learns visual concepts from data. Figure 8 shows examples of the learned visual concepts, including object categories, attributes, and relations. Experiment setup and implementation details are in Appendix F.2.

In this paper, we focus on a neuro-symbolic framework that learns visual concepts about object properties and relations. Indeed, visual question answering requires AI systems to reason about more general concepts such as events or activities (Levin, 1993). We leave the extension of NS-CL along this direction and its application to general VQA datasets (Antol et al., 2015) as future work.

## 5 Discussion and Future Work

We presented a method that jointly learns visual concepts, words, and semantic parsing of sentences from natural supervision. The proposed framework, NS-CL, learns by looking at images and reading paired questions and answers, without any explicit supervision such as class labels for objects. Our model learns visual concepts with remarkable accuracy. Based upon the learned concepts, our model achieves good results on question answering, and more importantly, generalizes well to new visual compositions, new visual concepts, and new domain specific languages.

The design of NS-CL suggests multiple research directions. First, constructing 3D object-based representations for realistic scenes needs further exploration (Anderson et al., 2018; Baradel et al., 2018). Second, our model assumes a domain-specific language for describing formal semantics. The integration of formal semantics into the processing of complex natural language would be meaningful future work (Artzi & Zettlemoyer, 2013; Oh et al., 2017). We hope our paper could motivate future research in visual concept learning, language learning, and compositionality.

Our framework can also be extended to other domains such as video and interactive domains. Here, we would need to discover semantic representations for actions and interactions (e.g., push) beyond static spatial relations. Along this direction, researchers have studied building symbolic representations for skills (Konidaris et al., 2018) and learning instruction semantics from interaction (Oh et al., 2017).

## REFERENCES


Omri Abend, Tom Kwiatkowski, Nathaniel J Smith, Sharon Goldwater, and Mark Steedman. Bootstrapping language acquisition. *Cognition*, 164:116–143, 2017.

Peter Anderson, Xiaodong He, Chris Buehler, Damien Teney, Mark Johnson, Stephen Gould, and Lei Zhang. Bottom-up and top-down attention for image captioning and visual question answering. In *CVPR*, 2018.

Jacob Andreas, Marcus Rohrbach, Trevor Darrell, and Dan Klein. Learning to compose neural networks for question answering. In *NAACL-HLT*, 2016.

Stanislaw Antol, Aishwarya Agrawal, Jiasen Lu, Margaret Mitchell, Dhruv Batra, C Lawrence Zitnick, and Devi Parikh. Vqa: Visual question answering. In *ICCV*, 2015.

Yoav Artzi and Luke Zettlemoyer. Weakly supervised learning of semantic parsers for mapping instructions to actions. *TACL*, 1:49–62, 2013.

Fabien Baradel, Natalia Neverova, Christian Wolf, Julien Mille, and Greg Mori. Object level visual reasoning in videos. In *ECCV*, 2018.

Kan Chen, Jiang Wang, Liang-Chieh Chen, Haoyuan Gao, Wei Xu, and Ram Nevatia. Abc-cnn: An attention based convolutional neural network for visual question answering. *arXiv preprint arXiv:1511.05960*, 2015.

Kyunghyun Cho, Bart Van Merriënboer, Caglar Gulcehre, Dzmitry Bahdanau, Fethi Bougares, Holger Schwenk, and Yoshua Bengio. Learning phrase representations using rnn encoder-decoder for statistical machine translation. In *EMNLP*, 2014.

Grzegorz Chrupała, Akos Kádár, and Afra Alishahi. Learning language through pictures. In *ACL*, 2015.

Jia Deng, Wei Dong, Richard Socher, Li-Jia Li, Kai Li, and Li Fei-Fei. Imagenet: A large-scale hierarchical image database. In *CVPR*, 2009.

Jeffrey Donahue, Lisa Anne Hendricks, Sergio Guadarrama, Marcus Rohrbach, Subhashini Venugopalan, Kate Saenko, and Trevor Darrell. Long-term recurrent convolutional networks for visual recognition and description. In *CVPR*, 2015.

Afsaneh Fazly, Afra Alishahi, and Suzanne Stevenson. A probabilistic computational model of cross-situational word learning. *Cognitive Science*, 34(6):1017–1063, 2010.

Chuang Gan, Yandong Li, Haoxiang Li, Chen Sun, and Boqing Gong. Vqs: Linking segmentations to questions and answers for supervised attention in vqa and question-focused semantic segmentation. In *ICCV*, 2017.

Siddha Ganju, Olga Russakovsky, and Abhinav Gupta. What's in a question: Using visual questions as a form of supervision. In *CVPR*, pp. 6422–6431. IEEE, 2017.

Jon Gauthier, Roger Levy, and Joshua B Tenenbaum. Word learning and the acquisition of syntactic–semantic overhypotheses. In *CogSci*, 2018.

Kaiming He, Xiangyu Zhang, Shaoqing Ren, and Jian Sun. Deep residual learning for image recognition. In *CVPR*, 2015.

Kaiming He, Georgia Gkioxari, Piotr Dollár, and Ross Girshick. Mask r-cnn. In *ICCV*, 2017.

Irina Higgins, Nicolas Sonnerat, Loic Matthey, Arka Pal, Christopher P Burgess, Matthew Botvinick, Demis Hassabis, and Alexander Lerchner. Scan: learning abstract hierarchical compositional visual concepts. In *ICLR*, 2018.

Ronghang Hu, Jacob Andreas, Trevor Darrell, and Kate Saenko. Explainable neural computation via stack neural module networks. In *ECCV*, 2018.

Drew A Hudson and Christopher D Manning. Compositional attention networks for machine reasoning. In *ICLR*, 2018.

Allan Jabri, Armand Joulin, and Laurens van der Maaten. Revisiting visual question answering baselines. In *ECCV*, 2016.

Justin Johnson, Ranjay Krishna, Michael Stark, Li-Jia Li, David Shamma, Michael Bernstein, and Li Fei-Fei. Image retrieval using scene graphs. In *CVPR*, 2015.

Justin Johnson, Andrej Karpathy, and Li Fei-Fei. Densecap: Fully convolutional localization networks for dense captioning. In *CVPR*, 2016.

Justin Johnson, Bharath Hariharan, Laurens van der Maaten, Li Fei-Fei, C Lawrence Zitnick, and Ross Girshick. Clevr: A diagnostic dataset for compositional language and elementary visual reasoning. In *CVPR*, 2017a.

Justin Johnson, Bharath Hariharan, Laurens van der Maaten, Judy Hoffman, Li Fei-Fei, C Lawrence Zitnick, and Ross Girshick. Inferring and executing programs for visual reasoning. In *ICCV*, 2017b.

Ryan Kiros, Ruslan Salakhutdinov, and Richard S Zemel. Unifying visual-semantic embeddings with multimodal neural language models. *arXiv preprint arXiv:1411.2539*, 2014.

George Konidaris, Leslie Pack Kaelbling, and Tomas Lozano-Perez. From skills to symbols: Learning symbolic representations for abstract high-level planning. *JAIR*, 61:215–289, 2018.

Tejas D Kulkarni, William F Whitney, Pushmeet Kohli, and Josh Tenenbaum. Deep convolutional inverse graphics network. In *NIPS*, 2015.

Beth Levin. *English verb classes and alternations*, volume 1. University of Chicago Press, 1993.

Tsung-Yi Lin, Michael Maire, Serge Belongie, James Hays, Pietro Perona, Deva Ramanan, Piotr Dollár, and C Lawrence Zitnick. Microsoft coco: Common objects in context. In *ECCV*, 2014.

M Malinowski and M Fritz. A multi-world approach to question answering about real-world scenes based on uncertain input. In *NIPS*, 2014.

Junhua Mao, Jiajing Xu, Kevin Jing, and Alan L Yuille. Training and Evaluating Multimodal Word Embeddings with Large-Scale Web Annotated Images. In *NIPS*, 2016.

David Mascharka, Philip Tran, Ryan Soklaski, and Arjun Majumdar. Transparency by design: Closing the gap between performance and interpretability in visual reasoning. In *CVPR*, 2018.

Tushar Nagarajan and Kristen Grauman. Attributes as operators: Factorizing unseen attribute-object compositions. In *ECCV*, 2018.

Junhyuk Oh, Satinder Singh, Honglak Lee, and Pushmeet Kohli. Zero-shot task generalization with multi-task deep reinforcement learning. In *ICML*, 2017.

Jeffrey Pennington, Richard Socher, and Christopher Manning. Glove: Global vectors for word representation. In *EMNLP*, pp. 1532–1543, 2014.

Ethan Perez, Florian Strub, Harm De Vries, Vincent Dumoulin, and Aaron Courville. Film: Visual reasoning with a general conditioning layer. *arXiv preprint arXiv:1709.07871*, 2017.

Adam Santoro, David Raposo, David GT Barrett, Mateusz Malinowski, Razvan Pascanu, Peter Battaglia, and Timothy Lillicrap. A simple neural network module for relational reasoning. In *NIPS*, 2017.

Sebastian Schuster, Ranjay Krishna, Angel Chang, Li Fei-Fei, and Christopher D Manning. Generating semantically precise scene graphs from textual descriptions for improved image retrieval. In *EMNLP Workshop*, 2015.

N Siddharth, T. B. Paige, J.W. Meent, A. Desmaison, N. Goodman, P. Kohli, F. Wood, and P. Torr. Learning disentangled representations with semi-supervised deep generative models. In *NIPS*, 2017.

Joseph Suarez, Justin Johnson, and Fei-Fei Li. Ddrprog: A clevr differentiable dynamic reasoning programmer. *arXiv:1803.11361*, 2018.

Ilya Sutskever, Oriol Vinyals, and Quoc V Le. Sequence to sequence learning with neural networks. In *NIPS*, 2014.

Richard S Sutton, David A McAllester, Satinder P Singh, and Yishay Mansour. Policy gradient methods for reinforcement learning with function approximation. In *NIPS*, 2000.

Ivan Vendrov, Ryan Kiros, Sanja Fidler, and Raquel Urtasun. Order-embeddings of images and language. In *ICLR*, 2016.

Ronald J Williams. Simple statistical gradient-following algorithms for connectionist reinforcement learning. *MLJ*, 8(3-4):229–256, 1992.

Jiajun Wu, Joshua B Tenenbaum, and Pushmeet Kohli. Neural scene de-rendering. In *CVPR*, 2017.

Huijuan Xu and Kate Saenko. Ask, attend and answer: Exploring question-guided spatial attention for visual question answering. In *ECV*, pp. 451–466. Springer, 2016.

Jimei Yang, Scott E Reed, Ming-Hsuan Yang, and Honglak Lee. Weakly-supervised disentangling with recurrent transformations for 3d view synthesis. In *NIPS*, 2015.

Zichao Yang, Xiaodong He, Jianfeng Gao, Li Deng, and Alex Smola. Stacked attention networks for image question answering. In *CVPR*, 2016.

Kexin Yi, Jiajun Wu, Chuang Gan, Antonio Torralba, Pushmeet Kohli, and Joshua B Tenenbaum. Neural-symbolic vqa: Disentangling reasoning from vision and language understanding. In *NIPS*, 2018.

Yukun Zhu, Ryan Kiros, Rich Zemel, Ruslan Salakhutdinov, Raquel Urtasun, Antonio Torralba, and Sanja Fidler. Aligning books and movies: Towards story-like visual explanations by watching movies and reading books. In *CVPR*, pp. 19–27, 2015.

# A CLEVR DOMAIN-SPECIFIC LANGUAGE AND IMPLEMENTATIONS

We begin the appendix with the introduction to a domain-specific language designed for the CLEVR VQA dataset (Johnson et al., 2017a).

| Operation Token | Signature | Description |
|---|---|---|
| `FilterScene` | Concept $\longrightarrow$ ObjectSet | Filter out a set of objects having the attribute Concept (e.g., red) from the scene. |
| `Filter` | ObjectSet, Concept $\longrightarrow$ ObjectSet | Filter out a set of objects having the attribute Concept (e.g., red) from the input object set. |
| `Relate` | Object, Concept $\longrightarrow$ ObjectSet | Filter out a set of objects that have the relation Concept (e.g., left) with the input object. |
| `AERelate` | Object, Attribute $\longrightarrow$ ObjectSet | Filter out a set of objects that have the same attribute value (e.g., same color) with the input object. |
| `Intersection` | ObjectSet, ObjectSet $\longrightarrow$ ObjectSet | Take the intersection of two object sets. |
| `Union` | ObjectSet, ObjectSet $\longrightarrow$ ObjectSet | Take the union of two object sets. |
| `Query` | Object, Attribute $\longrightarrow$ Concept | Query the attribute (e.g., color) of the input object. |
| `AEQuery` | Object, Object, Attribute $\longrightarrow$ Bool | Query if two input objects have the same attribute value (e.g., same color). |
| `Count` | ObjectSet $\longrightarrow$ Integer | Query the number of objects in a set. |
| `LessThan` | ObjectSet, ObjectSet $\longrightarrow$ Bool | Query if the number of objects in the first input set is less than the one of the second set. |
| `GreaterThan` | ObjectSet, ObjectSet $\longrightarrow$ Bool | Query if the number of objects in the first input set is greater than the one of the second set. |
| `Equal` | ObjectSet, ObjectSet $\longrightarrow$ Bool | Query if the number of objects in the first input set is the same as the one of the second set. |

Table 6: The domain specific language for CLEVR VQA.

We note that some function takes Object as its input instead of ObjectSet. These functions require the uniqueness of the referral object. For example, to answer the question "What's the color of the red object?", there should be one and only one red object in the scene. During the program execution, the object sets will be implicitly casted to the single object (if valid) using a special operation called `Unique`.

We adopt a quasi-symbolic implementation of object sets. Denote the set of all objects in the scene as a set $S$, we represent a subset $T \subseteq S$ by assigning a real value for each object $\in S$, denoting the probability that the specific object belongs to $T$. We call such representations "masks" on all objects.

# B SEMANTIC PARSING

We adopt a visually-grounded semantic parsing approach for the joint learning of visual concepts, word semantics and semantic parsing of sentences. We consider three types of visually-grounded words:

**Object-level concepts.** This group includes red, blue, cube, sphere, big, small, rubber, material, etc.

**Relation-level concepts.** This group includes front, behind, left and right.

**Visual attributes.** This group includes color, shape, material and size.

Here we add a small note for reproducibility: in the CLEVR dataset, some object-level concepts have synonyms (e.g., box is a synonym of cube). We also consider their synonyms as independent concepts.

The goal of the language module is to learn the word semantics of concept words and the semantic parsing of sentences of different forms. Consider the sentence "What is the color of the cube right of the red matte object?". To exploit the grounded nature of natural language questions, in our DSL, we treat visual concepts and attributes such as `Color` or `Cube` in the above case as parameters of program operations, instead of part of the program token as in Johnson et al. (2017b) or Mascharka et al. (2018). We impose the restriction that all such parameters in the program must be chosen from the set of concept words appeared in the sentence.

Another pre-processing to the sentence is to group consecutive concept words into a group and treat it as a single concept. The intuition behind this grouping is, the latent programs of CLEVR questions usually contain multiple consecutive `Filter` tokens. In the program execution, we want to fuse all such `Filter`s into a single `Filter` operation that takes multiple concepts as its parameter.

Consider again the sentence "What is the color of the cube right of the red matte object?". We encode the sentence as: "What is the <attribute 1> of the <concept 1> <relational concept 1> of the <concept 2>", where each concept is marked with a special label indicating their type. The expected parsing result of this sentence is:

```
Query(<attribute 1>, Filter(<concept 1>,
      Relate(<relational concept 1>, Filter-Scene(<concept 2>) )
) ).
```

We generate the hierarchical program structure using a sequence-to-sequence-like model based on the encoder-decoder architecture. We fill in the parameters of each token using the attention on the input sequence, chosen from all concept words in the sentence. Algorithm 1 illustrates the algorithm outline of the semantic parsing.

**Algorithm 1:** String-to-Tree Semantic parser.

**Function** `parse` $(f_s, \{c_i\})$ **:**
- $program \leftarrow$ `EmptyProgram`();
- $program.op \leftarrow$ `OpDecoder`$(f_s)$;
- **if** *program requires concept parameter* **then**
  - $program.concept \leftarrow$ `ConceptDecoder`$(f_s, \{c_i\})$;
- **for** $i = 0, 1, \cdots$ number of parameters **do**
  - $program.param[i] \leftarrow$ `parse` ( `ParamDecoder`$_i(f_s, program.op)$ ,$\{c_i\}$ );
- **return** $program$

Shown in Algorithm 1, we first map each word into a word embedding space of dimension $256$. We concatenate the word embedding with a positional embedding of dimension $128$. The semantic parser begins with a two-layer GRU with a hidden dimension of $256 * 2$ (bidirectional). The function `Parse` starts from the state encoded by the GRU, and works recursively to generate the hierarchical program layout. Parameter decoder $0$ and $1$ are individual GRU cells. `ConceptDecoder` performs attention using current state $f_s$ over all encoded feature of concept words by the GRU. We select (sample) the concept word as parameters based on the attention weights.

**Off-policy program search.** To tackle the optimization in a non-smooth program space, we apply an off-policy program search process(Sutton et al., 2000) to assist the REINFORCE for training the semantic parser. Denote $\mathbb{P}(s)$ as the set of all valid programs in the CLEVR dataset with parameters chosen from concepts in the sentence $s$. We want to compute the gradient w.r.t. $\Theta_s$, which requires summing over all possible $p \in \mathbb{P}(s)$. In REINFORCE, we approximate it via Monte Carlo sampling.

An alternative solution is to exactly compute the gradient. Note in Equation 1, only the set of programs $\mathbb{Q}(s)$ leading to correct answer will contribute to the gradient estimation. With the perception module fixed, the set $\mathbb{Q}$ can be determined by an off-policy exhaustive search. In the third stage, we search for the set $\mathbb{Q}$ offline and compute the exact gradient $\nabla\Theta_s$ during training. An intuitive explanation of the off-policy search is that, we search over all possible programs and find the ones leading to the correct answer. We use $\mathbb{Q}(s)$ as the program annotation for the question.

**Spurious program suppression.** However, directly using $\mathbb{Q}(s)$ as the annotations for the supervision as $\ell = \sum_{p\in\mathbb{Q}(S)} -\log \Pr(p)$ can be problematic, due to the spuriousness or ambiguity of the programs. This comes from two aspects: 1) intrinsic ambiguity: two programs are different but equivalent. For example $\texttt{color-equal-query}(\texttt{filter}(\texttt{cube}), \texttt{filter}(\texttt{sphere}))$ is equivalent to $\texttt{exist}(\texttt{filter}(\texttt{sphere}, \texttt{color-equal-relate}(\texttt{filter}(\texttt{cube}))))$. 2) extrinsic spuriousness: the program is incorrect, but may lead to correct answer under a specific scene. For example, although the correct understanding might be "the red object behinds the cube", interpret the sentence as "the red object behinds the sphere" may also locate the correct red object being referred to. To suppress such spurious programs, we change the loss function as: $\ell = \sum_{p\in\mathbb{Q}} \Pr[p] \cdot (-\log \Pr[p])$. The key observation is that, given a sufficiently large set of scenes, a program can be identified as spurious if there exists at least one scene where the program leads to a wrong answer. As the training goes, such spurious programs will get less update due to the sample importance term $\Pr[p]$ which weights the likelihood maximization term.

## C PROGRAM EXECUTION

Table 7 summarizes the implementation of some representative operators.

| Opeartor | Signature | Implementation |
|---|---|---|
| FilterScene | $\texttt{Concept} \rightarrow \texttt{Mask}^o$ | $\texttt{Mask}_i^o = \texttt{Concept}_i$ |
| Filter | $\texttt{Mask}, \texttt{Concept} \rightarrow \texttt{Mask}^o$ | $\texttt{Mask}_i^o = \min(\texttt{Mask}_i, \texttt{Concept}_i)$ |
| Relate | $\texttt{Mask}, \texttt{RConcept} \rightarrow \texttt{Mask}^o$ | $\texttt{Mask}_i^o = \sum_j (\texttt{Mask}_j \cdot \texttt{RConcept}_{j,i})$ |
| Intersection | $\texttt{Mask}^1, \texttt{Mask}^2 \rightarrow \texttt{Mask}^o$ | $\texttt{Mask}_i^o = \min(\texttt{Mask}_i^1, \texttt{Mask}_i^2)$ |
| Union | $\texttt{Mask}^1, \texttt{Mask}^2 \rightarrow \texttt{Mask}^o$ | $\texttt{Mask}_i^o = \max(\texttt{Mask}_i^1, \texttt{Mask}_i^2)$ |
| Unique | $\texttt{Mask} \rightarrow \texttt{Mask}^o$ | $\texttt{Mask}_i^o = \mathbf{1}[i = \arg\max \texttt{Mask}]$ |
| Query | $\texttt{Mask}, \texttt{Attr} \rightarrow \texttt{Concept}^o$ | $\texttt{Concept}^o = \arg\max_{c\in\texttt{Attr}} \sum \texttt{Mask}_i \cdot c_i$ |
| Count | $\texttt{Mask} \rightarrow \texttt{Integer}$ | $\texttt{Integer} = \sum_i \texttt{Mask}_i$ |
| Exist | $\texttt{Mask} \rightarrow \texttt{Bool}$ | $\texttt{Bool} = \max_i \texttt{Mask}_i$ |

Table 7: Our program executor takes an quasi-symbolic way to execute programs.

We implement a set of generic operations for VQA. The LHS in the signature column are the inputs while the RHS the output. Each `Mask` is a real-valued vector denoting an object set. Throughout this section, we consider a scene containing $n$ objects.

Take `Filter` as an example, it takes the current set of objects, represented by a vector `Mask` of length $n$, with each value $\texttt{Mask}_i$ representing the probability that the $i$-th object belongs to the set and a concept word (e.g., `Cube`) as input. We compute a probability vector `Concept` that $\texttt{Concept}_i$ denotes the probability that object $i$ is a `Cube`. The output of the filter operation is still a object set, represented by a vector $\texttt{Mask}^{(o)}$, where $\texttt{Mask}_i^{(o)} = \min(\texttt{Mask}_i, \texttt{Concept}_i)$.

Sharing a similar spirit, the `Relate` operation is implemented by computing an $n \times n$ matrix `RConcept` based on the input relational concept (e.g., `Left`), where $\texttt{RConcept}_{j,i}$ denotes the probability that object $i$ is left of object $j$ in the scene.

Unique is a special operation use for transforming an object set into a single object. During the inference, this operation is simply choosing the object $i$ having the highest score: $i = \arg\max_j \texttt{Mask}_j$. During the training, this operation is implemented by taking the softmax.

To query the attribute (e.g., `Shape`) of an object, we first enumerate all concepts belongs to this attribute (e.g., `Cube`, `Sphere`, `Cylinder`), and computes the probability that the object is of each kind of shapes. During the inference, we answer the query by the most confident prediction, while during the training, we take the softmax.

# D CURRICULUM LEARNING SETUP

During the whole training process, we gradually add more visual concepts and more complex question examples into the model. Summarized in Figure 4(A), in general, the whole training process is split into 4 stages. First, we only use questions from lesson 1 to let the model learn object-level visual concepts. Second, we train the model to parse simple questions (with depth $\leq 4$) and to learn relational concepts. Here we freeze the neural operators and embeddings of object-level concepts. Third, we fix all perception modules. The model gets trained on the full question set (lesson 3), learning to understand questions of different complexities and various format. Finally, at the last stage, we finetune all modules.

We select questions for each lesson in the curriculum learning by their depth of the latent program layout. For eaxmple, the program "`Query(Shape, Filter-Scene(Red))`" has the depth of 2, while the program "`Query(Shape Filter(Cube, Relate(Left, Filter-Scene(Red))))`" has the depth of 4. We fuse the consecutive `Filter` operations into a single one, taking a group of concepts as input. We also fuse `Attribute-Equal-Query` and `Query`, `Less-Than` and `Count` into a same operator. We compute the depth based on the fused program. Thus, the maximum depth of all programs is 8 on the CLEVR dataset.

We now present the split of our curriculum learning lessons.

For lesson 1, we introduce only programs of depth 2. It contains three types of questions: querying an attribute of the object, querying the existence of a certain type of objects, count a certain type of objects, and querying if two objects have the same attribute (e.g., of the same color). These questions are almost about fundamental object-based visual concepts.

For lesson 2, we introduce programs of depth less than 4, containing a number of relation-typed questions such as querying the attribute of an object that is left of another object. We found that in the original CLEVR dataset, all `Relate` operations are followed by a `Filter` operation. This setting degenerates the performance of the learning of relational concepts such as `Left`. Thus, we manually add another question type: `Count(Relate(Filter-Scene()))` (e.g., "What's the number of objects that are left of the cube?") to facilitate the learning of relational concepts.

For lesson 3, we use the full set of CLEVR question set.

# E ABLATION STUDY

## E.1 PROGRAM ACCURACY.

We also evaluate how well our model recovers the underlying programs of questions. Due to the intrinsic equivalence of different programs, we evaluate the accuracy of programs by executing them on the ground-truth annotations of objects. Invalid or ambiguous programs are also considered as incorrect. Our semantic parser archives $> 99.9\%$ QA accuracy on the validation split.

## E.2 IMPACTS OF THE IMAGENET PRE-TRAINING.

The only extra supervision of the visual perception module comes from the pre-training of the perception modules on ImageNet Deng et al. (2009). To quantify the influence of this pre-training, we conduct ablation experiments where we randomly initialize the perception module following He et al. (2015). The classification accuracies of the learned concepts almost remain the same except for `Shape`. The classification accuracy of `Shape` drops from 98.7 to 97.5 on the validation set while the overall QA accuracy on the CLEVR dataset drops to 98.2. We speculate that large-scale image recognition dataset can provide prior knowledge of shape.

## E.3 DATA EFFICIENCY AND OBJECT-BASED REPRESENTATIONS

In this section, we study whether and how the number of training samples and feature representations affect the overall performance of various models on the CLEVR dataset. Specifically, we compare the proposed NS-CL against two strong baselines: TbD (Mascharka et al., 2018) and MAC (Hudson & Manning, 2018).

**Baselines.** For comparison, we implement two variants of the baseline models: TbD-Object and MAC-Object. Inspired by Anderson et al. (2018), instead of using a 2D convolutional feature map, TbD-Object and MAC-Object take a stack of object features as inputs, whose shape is $k \times d_{obj}$. $k$ is the number of objects in the scene, and $d_{obj}$ is the feature dimension for a single object. In our

experiments, we fix $k = 12$ as a constant value. If there are fewer than 12 objects in the scene, we add "null" objects whose features are all-zero vectors.

We extract object features in the same way as NS-CL. Features are extracted from a pre-trained ResNet-34 network before the last residual block for a feature map with high resolution. For each object, its feature is composed of two parts: region-based (by RoI Align) and image-based features. We concatenate them to represent each object. As discussed, the inclusion of the representation of the full scene is essential for the inference of relative attributes such as size or spatial position on the CLEVR domain.

TbD and MAC networks are originally designed to use image-level attention for reasoning. Thus, we implement two more baselines: TbD-Mask and MAC-Mask. Specifically, we replace the original attention module on images with a mask-guided attention. Denotes the union of all object masks as $M$. Before the model applies the attention on the input image, we multiply the original attention map computed by the model with this mask $M$. The multiplication silences the attention on pixels that are not part of any objects.

**Results.** Table 3 summarizes the results. We found that TbD-Object and MAC-Object approach show inferior results compared with the original model. We attribute this to the design of the network architectures. Take the `Relate` operation (e.g., finds all objects left of a specific object $x$) as an example. TbD uses a stack of dilated convolutional layers to propagate the attention from object $x$ to others. In TbD-Object, we replace the stack of 2D convolutions by several 1D convolution layers, operating over the $k \times d_{obj}$ object features. This ignores the equivalence of objects (the order of objects should not affect the results). In contrast, MAC networks always use the attention mechanism to extract information from the image representation. This operation is invariant to the order of objects, but is not suitable for handling quantities (e.g., counting objects).

As for TbD-Mask and MAC-Mask, although the mask-guided attention does not improve the overall performance, we have observed noticeably faster convergence during model training. TbD-Mask and MAC-Mask leverage the prior knowledge of object masks to facilitate the attention. Such prior has also been verified to be effective in the original TbD model: TbD employs an attention regularization during training, which encourages the model to attend to smaller regions.

In general, NS-CL is more data-efficient than MAC networks and TbD. Recall that NS-CL answers questions by executing symbolic programs on the learned visual concepts. Only visual concepts (such as `Red` and `Left`) and the interpretation of questions (how to translate questions into executable programs) need to be learned from data. In contrast, both TbD and MAC networks need to additionally learn to execute (implicit or explicit) programs such as counting.

For the experiments on the full CLEVR training set, we split 3,500 images (5% of the training data) as the hold-out validation set to tune the hyperparameters and select the best model. We then apply this model to the CLEVR validation split and report the testing performance. Our model reaches an accuracy of 99.2% using the CLEVR training set.

# F Extending to Other Scene and Language Domains

## F.1 Minecraft Dataset

We also extend the experiments to a new reasoning testbed: Minecraft worlds (Yi et al., 2018). The Minecraft reasoning dataset differs from CLEVR in both visual appearance and question types. Figure 9 gives an example instance from the dataset.

**Q**: What direction is the closest creature facing?
**A**: Left.
**P**: Query(Direction, FilterMost(Closest,
Filter(Creature)
))

Figure 9: An example image and a related question-answering pair from the Minecraft dataset.

**Setup.** Following Yi et al. (2018), we generate 10,000 Minecraft scenes using the officially open-sourced tools by Wu et al. (2017). Each image contains 3 to 6 objects. The objects are chosen from 12 categories, with 4 different facing directions (front, back, left and right). They stand on a 2D plane.

Besides different 3D visual appearance and image contexts, the Minecraft reasoning dataset introduces two new types of reasoning operations. We add them to our domain-specific language:

1. `FilterMost`(ObjectSet, Concept) → ObjectSet: Given a set of objects, finds the "most" one. For example, `FilterMost`(`Closest`, set) locates the object in the input set that is cloest to the camera (e.g., what is the direction of the closest animal?)
2. `BelongTo`(Object, ObjectSet) → Bool: Query if the input object belongs to a set.

**Results.** Table 8 summarizes the results and Figure 12 shows sample execution traces. We compare our method against the NS-VQA baseline (Yi et al., 2018), which uses strong supervision for both scene representation (e.g., object categories and positions) and program traces. In contrast, our method learns both by looking at images and reading question-answering pairs. NS-CL outperforms NS-VQA by 5% in overall accuracy. We attribute the inferior results of NS-VQA to its derendering module. Because objects in the Minecraft world usually occlude with each other, the detected object bounding boxes are inevitably noisy. During the training of the derendering module, each detected bounding box is matched with one of the ground-truth bounding boxes and uses its class and pose as supervision. Poorly localized bounding boxes lead to noisy labels and hurt the accuracy of the derendering module. This further influences the overall performance of NS-VQA.

| Model | Overall | Count | Exist | Belong | Query |
|---|---|---|---|---|---|
| NS-VQA | 87.7 | 83.3 | 91.5 | 91.1 | 86.4 |
| NS-CL | **93.3** | **91.3** | **95.6** | **93.9** | **94.3** |

Table 8: Our model achieves comparable results on the Minecraft dataset with baselines trained by full program annotations.

### F.2 VQS Dataset

We conduct experiments on the VQS dataset (Gan et al., 2017). VQS is a subset of the VQA 1.0 dataset (Antol et al., 2015). It contains questions that can be visually grounded: each question is associated with multiple image regions, annotated by humans as necessary for answering the question.

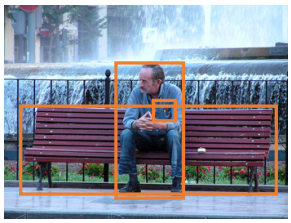

**Q**: Does this man have any pens on him?
**A**: Yes.
**P**: Exist(Filter(Man,
Relate(Have, Filter(Pen))
))

Figure 10: An example image from the VQS dataset. The orange bounding boxes are object proposals. On the right, we show the original question and answer in natural language, as well as the latent program recovered by our parser. To answer this question, models are expected to attend to the man and his pen in the pocket.

**Setup.** All models are trained on the first 63,509 images of the training set, and tested on the test split. For hyper-parameter tuning and model selection, the rest 5,000 images from the training set are used for validation. We use the multiple-choice setup for VQA: the models choose their most confident answer from 18 candidate answers for each question.

To obtain the latent programs from natural languages, we use a pre-trained syntactic dependency parser (Andreas et al., 2016; Schuster et al., 2015) for extracting programs and concepts that need to be learned. A sample question and the program obtained by our parser is shown in Figure 10. The concept embeddings are initialized by the bag of words (BoW) over the GloVe word embeddings Pennington et al. (2014).

**Baselines.** We compare our model against two representative baselines: MLP (Jabri et al., 2016) and MAC (Hudson & Manning, 2018).

MLP is a standard baseline for visual-question answering, which treats the multiple-choice task as a ranking problem. For a specific candidate answer, a multi-layer perceptron (MLP) model is used to encode a tuple of the image, the question, and the candidate answer. The MLP outputs a score for each tuple, and the answer to the question is the candidate with the highest score. We encode the image with a ResNet-34 pre-trained on ImageNet and use BoW over the GloVe word embeddings for the question and option encoding.

We slightly modify the MAC network for the VQS dataset. For each candidate answer, we concatenate the question and the answer as the input to the model. The MAC model outputs a score from 0 to 1 and the answer to the question is the candidate with the highest score. The image features are extracted from the same ResNet-34 model.

**Results.** Table 7 summarizes the results. NS-CL achieves comparable results with the MLP baseline and the MAC network designed for visual reasoning. Our model also brings transparent reasoning over natural images and language. Example execution traces generated by NS-CL are shown in Figure 13. Besides, the symbolic reasoning process helps us to inspect the model and diagnose the error sources. See the caption for details.

## G VISUALIZATION OF EXECUTION TRACES AND VISUAL CONCEPTS

Another appealing benefit is that our reasoning model enjoys full interpretability. Figure 11, Figure 12, and Figure 13 show NS-CL's execution traces on CLEVR, Minecraft, and VQS, respectively. As a side product, our system detects ambiguous and invalid programs and throws out exceptions. As an example (Figure 11), the question "What's the color of the cylinder?" can be ambiguous if there are multiple cylinders or even invalid if there are no cylinders.

Figure 14 and Figure 15 include qualitative visualizations of the concepts learned from the CLEVR and Minecraft datasets, including object categories, attributes, and relations. We choose samples from the validation or test split of each dataset by generating queries of the corresponding concepts. We set a threshold to filter the returned images and objects. For quantitative evaluations of the learned concepts on the CLEVR dataset, please refer to Table 2 and Table 5.

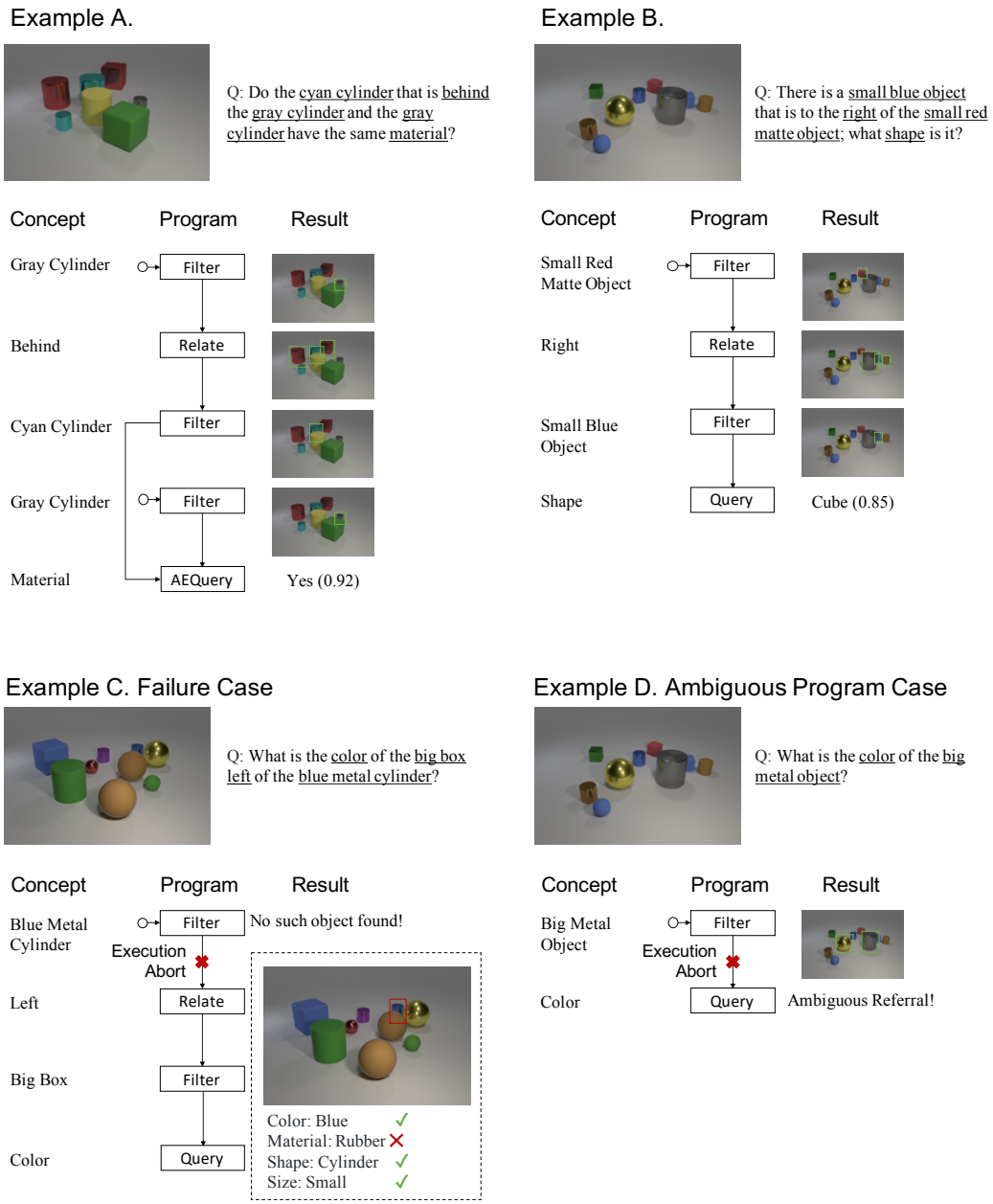


Figure 11: Visualization of the execution trace generated by our Neuro-Symbolic Concept Learner on the CLEVR dataset. Example A and B are successful executions that generate correct answers. In example C, the execution aborts at the first operator. To inspect the reason why the execution engine fails to find the corresponding object, we can read out the visual representation of the object, and locate the error source as the misclassification of the object material. Example D shows how our symbolic execution engine can detect invalid or ambiguous programs during the execution by performing sanity checks.

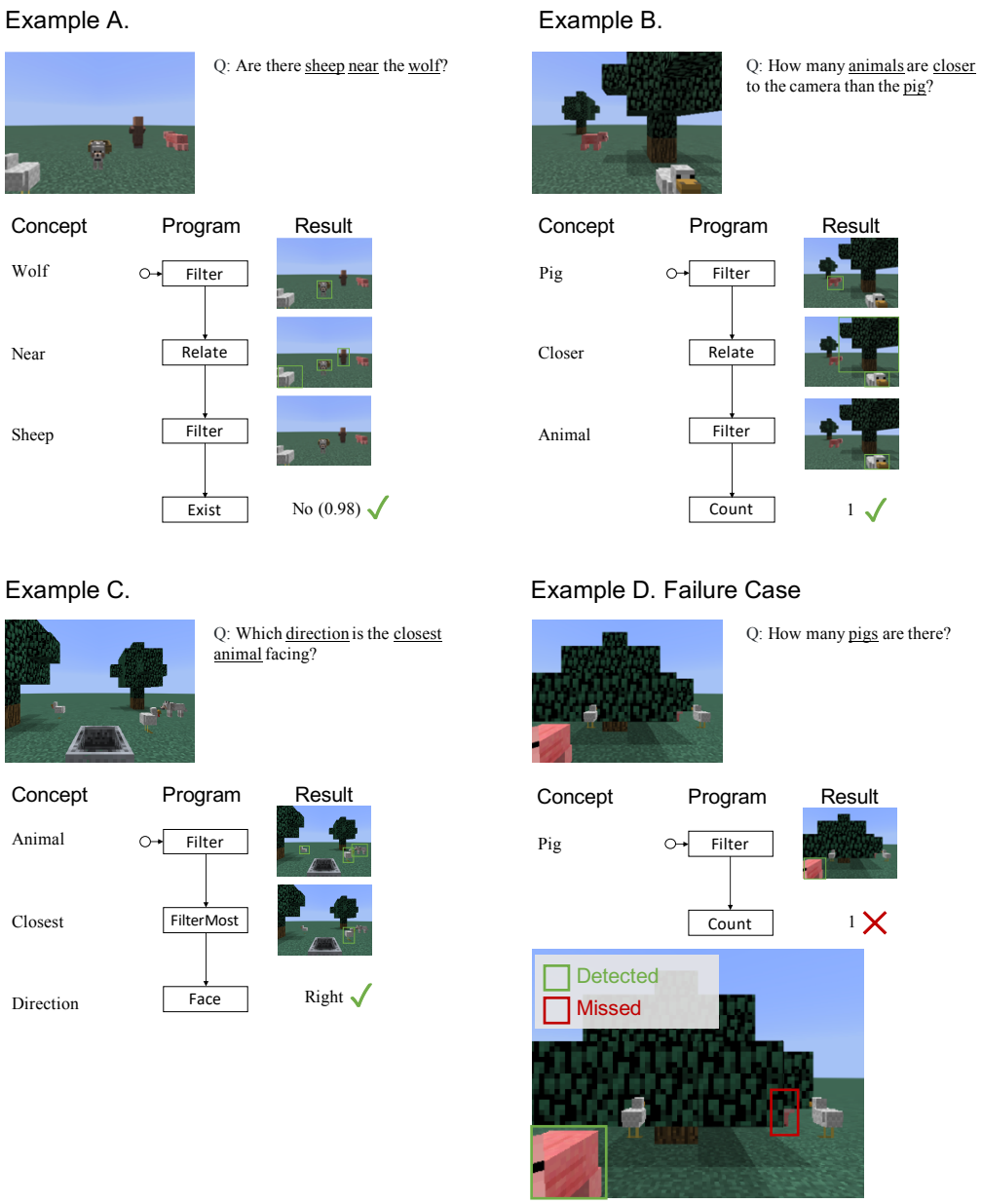


Figure 12: Exemplar execution trace generated by our Neuro-Symbolic Concept Learner on the Minecraft reasoning dataset. Example A, B and C are successful execution. Example C demonstrates the semantics of the FilterMost operation. Example D shows a failure case: the detection model fails to detect a pig hiding behind the big tree.

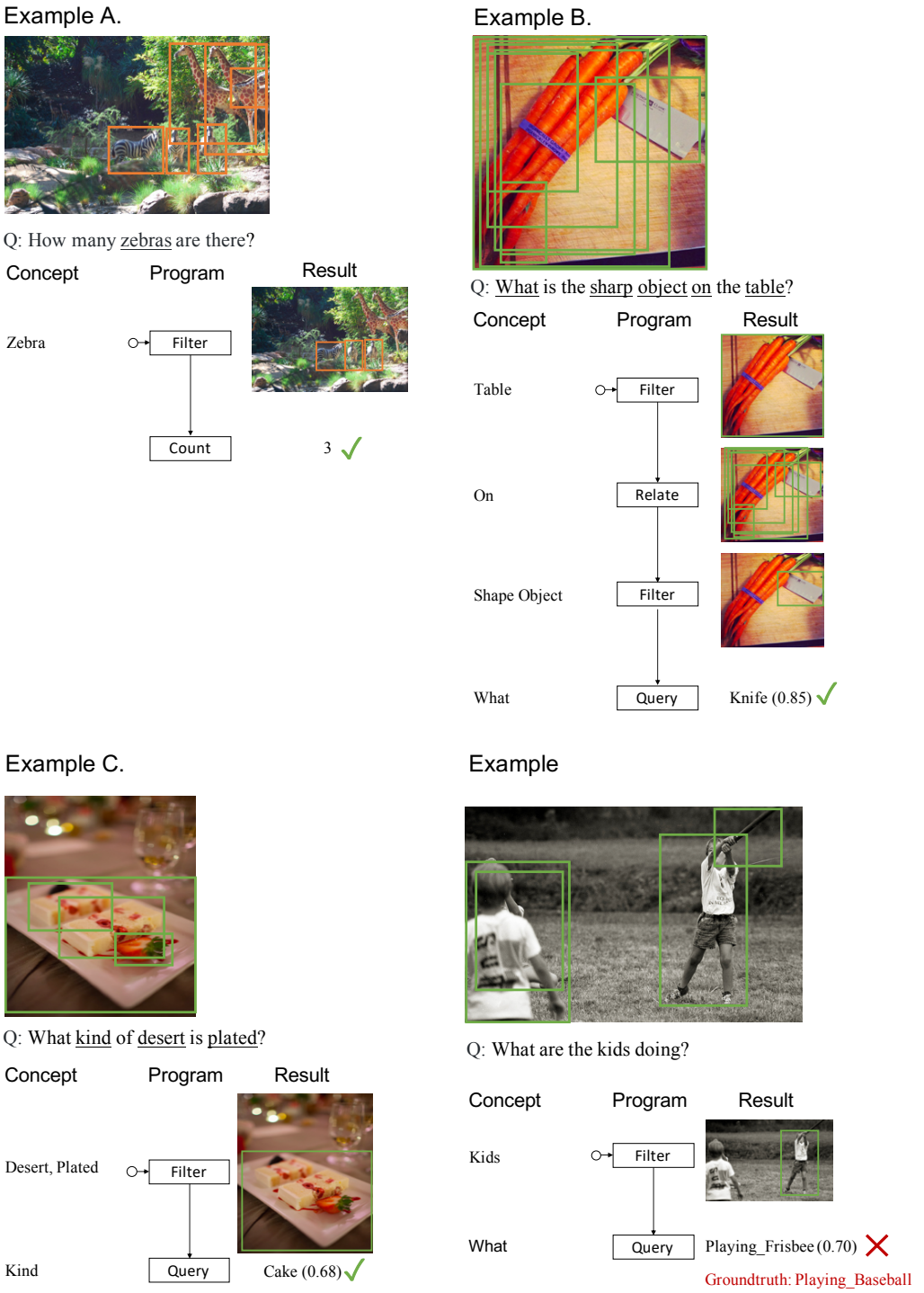


Figure 13: Illustrative execution trace generated by our Neuro-Symbolic Concept Learner on the VQS dataset. Execution traces A and B shown in the figure leads to the correct answer to the question. Our model effectively learns visual concepts from data. The symbolic reasoning process brings transparent execution trace and can easily handle quantities (e.g., object counting in Example A). Example C and D show two failure execution traces generated by our Neuro-Symbolic Concept Learner on the VQS dataset. In Example E, although NS-CL answers the question correctly, it locates the wrong object during reasoning: a dish instead of the cake. In Example F, our model misclassifies the sport as frisbee.

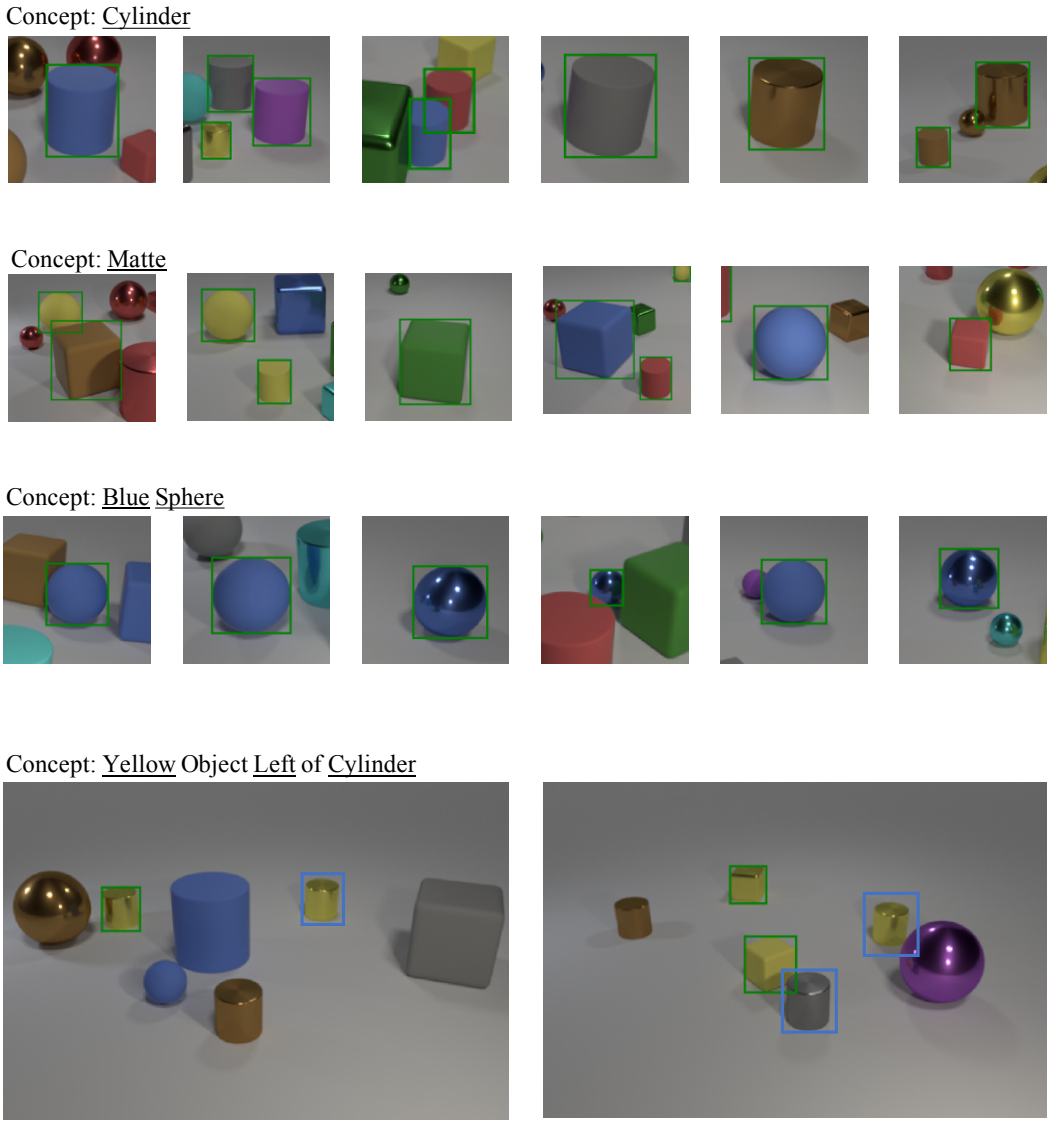


Figure 14: Concepts learned on the CLEVR dataset.

Concept: Wolf

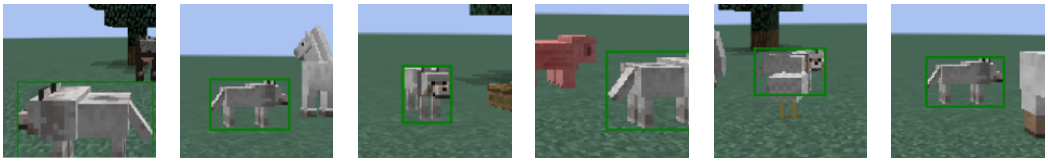

Concept: Animal That Faces Right

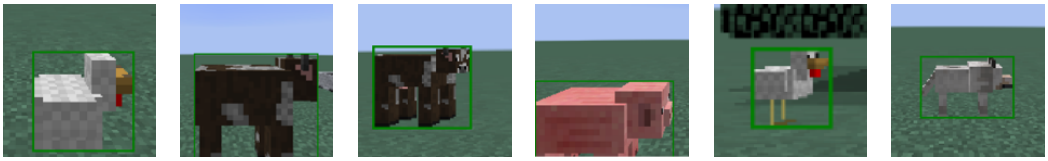

Concept: Closest Living Thing

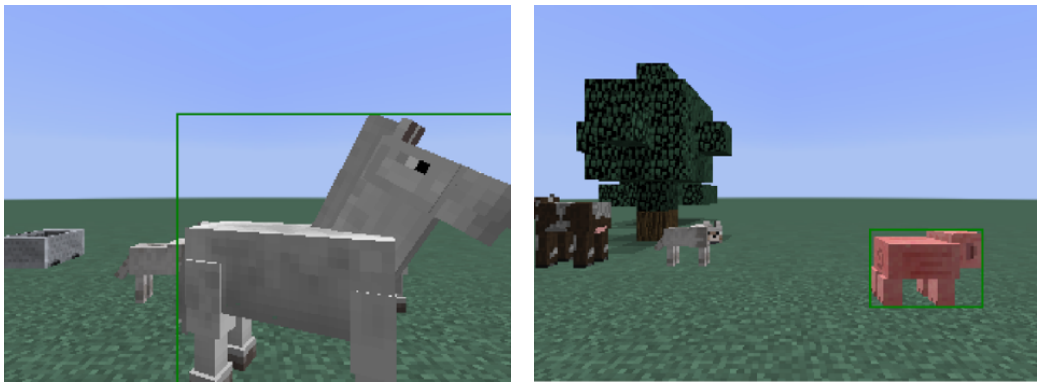

Concept: Villager Closer Than Pig

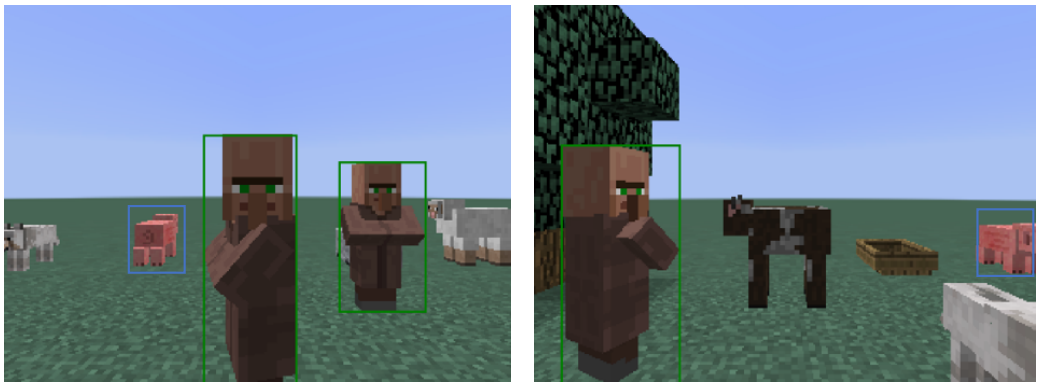

Figure 15: Concepts learned on the Minecraft dataset.